

## Computation of the Three-dimensional Depletion Approximation by Newton's Method and Multigrid

Franklin Bodine, Michael Holst and Thomas Kerkhoven

Beckman Institute and Department of Computer Science  
University of Illinois at Urbana-Champaign  
Urbana, IL 61801,  
USA

### Abstract

The three-dimensional (3D) depletion approximation is computed numerically by solution of a modified version of Poisson's equation for the electrostatic potential. Nonlinearities are resolved by a globally convergent modification of Newton's method. The linear systems are solved by 3D multigrid routines.

### I. Introduction

Computational algorithms to resolve the nonlinearities in numerical drift-diffusion modeling such as Newton's or Gummel's method generally require a reasonably accurate initial guess. The charge neutral approximation provides one possible option that is obtained with little computational effort. An alternative approximate solution is provided by the depletion approximation, which tends to be presented in the context of analytical one-dimensional modeling. In this paper we present numerical results obtained with a novel computational multi-dimensional implementation of the depletion approximation.

If  $q$  is the size of the electron charge,  $T$  the ambient temperature, and  $k_B$  Boltzmann's constant, then the thermal potential  $U_T \equiv (k_B T)/q$ . The intrinsic Debye length  $\lambda_{D,i}$  is then equal to  $\lambda_{D,i} \equiv \sqrt{(\epsilon_r \epsilon_0 k_B T)/(q^2 n_i)}$ . We express length in terms of an arbitrary unit  $l_0$ . The nonlinear Poisson equation, in terms of the electrostatic potential  $u$  (in units of the thermal  $U_T$ ) and the quasi-Fermi levels  $v$  and  $w$ , is then given by

$$-\nabla^2 u + \left(\frac{l_0}{\lambda_{D,i}}\right)^2 [e^{u-v} - e^{w-u} - k_1] = 0. \quad (1)$$

In thermal equilibrium the quasi-Fermi levels  $v$  and  $w$  may be set equal to the constant value 0. In the charge-neutral approximation the potential function  $u$  is set equal to

$$u_{cn} \equiv \sinh^{-1}(k_1/2). \quad (2)$$

However, it is obvious that the charge neutral approximation  $u_{cn}$  is significantly less accurate as an estimate to the solution  $u$  to Eq. (1) if  $v$  and  $w$  vary significantly, reflecting applied bias potentials. The charge-neutral approximation will be particularly inaccurate in modeling the depletion around reverse biased p-n junctions.

Our algorithm to compute the multi-dimensional depletion approximation employs a modification of the nonlinear Poisson equation (1) in which we attempt to reduce mobile charge

densities to 0 where the solution is furthest from thermodynamic equilibrium. The modified Poisson equation is given by

$$-\nabla^2 u_{depl} + \left(\frac{l_0}{\lambda_{D,i}}\right)^2 [(e^{u_{depl}-v_{pc}} - e^{w_{pc}-u_{depl}}) * e^{-\sqrt{(u_{depl}-v_{pc}-(u_{te}-v_{te})^2+1}+1} - k_1] = 0 \quad (3)$$

where  $u_{depl}$  is the potential distribution which accounts for all depletion,  $v_{pc}$  and  $w_{pc}$  are the piece-wise constant quasi-Fermi levels,  $u_{te}$  is the thermal equilibrium potential distribution, and  $v_{te}$  is the quasi-Fermi level in thermal equilibrium (which is zero). The nonlinearities are resolved with Newton's method and the linear systems are solved with three-dimensional multigrid routines developed by the second author [1]. Special care was taken to keep the linear systems well-conditioned. First, we solve Eq. (1) without externally applied bias for  $u_{te}$ . Then the externally applied biases are applied at the contacts. The quasi-Fermi levels are adjusted in a piece-wise constant manner in each doping region to match the applied bias for the contact on that region. Then Eq. (3) is solved for the complete depletion.

## II. Numerical Software

The linear multilevel method at the core of the software, as described in [1, 2], allows for discontinuous coefficients as occur in material interface problems. Operator-induced prolongation procedures are used to enforce flux conservation at box boundaries when a mesh function is interpolated from a coarse to a fine mesh. Smoothing operators are Red/Black Gauss-Seidel and weighted Jacobi, whereas the coarse mesh problem is solved with conjugate gradient methods. Nonlinear problems are handled with an extremely robust globally convergent damped-inexact-Newton-multilevel solver based on fast linear multilevel methods for the inexact Jacobian system solves. A nonlinear prolongation operator has been employed for nested Newton iteration. The discretization is with the box method.

To handle the severe numerical problems occurring with nonlinearities of exponential-type present in the semiconductor equations, we developed argument-capping functions which avoid nonvectorizable statements. Calls to the standard intrinsic functions are replaced by these modified functions, and overflows are successfully avoided during early transient iterations without losing the execution efficiency of the intrinsic functions. Due to the various choices made during the development of this package, the software executes at very high rates on a number of modern computers; see for example [1, 2] for benchmarks.

## III. Numerical Results

In the following pages, we show the initial charge neutral, Fig. 1, the thermal equilibrium, Fig. 2, and the final depleted, Fig. 3, electron depletion for a three-dimensional BJT model. The computational grid was  $49 \times 49 \times 25$  yielding a total of 60,025 unknowns. The computation of the our depletion model took 48 seconds on a HP 735 workstation, demonstrating the considerable computational efficiency of the multigrid routines.

Figures 1, 2, and 3 show two cut planes, one on the top on the of the device and one down the middle. The emitter is near the center, but slightly to the left, the base contact

Table 1: Timing and Iteration Statistics

Grid Size	Number of Points	Solution Time	Newton Iterations Thermal Equil.	Newton Iterations Applied Bias
25 × 25 × 25	15,625	15.02	5	6
25 × 25 × 33	20,625	20.04	5	6
33 × 33 × 33	35,937	40.16	5	7
49 × 49 × 33	79,233	103.07	6	7
49 × 49 × 49	117,649	152.23	6	7

is to the right of the emitter, and the collector contact is near the right edge. The lighter areas of the planes, representing lower electron densities ( $\leq 5 \times 10^{16} \text{ cm}^{-3}$ ), are the parts of the base and collector which have been depleted of electrons.

The device simulated is a BJT built in an area of  $1 \mu\text{m} \times 1 \mu\text{m}$  which is  $0.5 \mu\text{m}$  deep. The device has a realistic doping profile [3, 4]. The background n-doping of  $10^{17} \text{ cm}^{-3}$  forms the collector. The base has a  $0.46 \mu\text{m} \times 0.50 \mu\text{m}$  surface area and a depth of  $0.15 \mu\text{m}$  with a p-type doping of  $10^{18} \text{ cm}^{-3}$ . The n-type emitter, which is doped at  $10^{20} \text{ cm}^{-3}$ , has a  $0.08 \mu\text{m} \times 0.13 \mu\text{m}$  area and a depth of  $0.04 \mu\text{m}$ . This base width corresponds closely to [5].

The Debye length is given by [6],  $L_D = \sqrt{(\epsilon_r \epsilon_0 k_B T) / (q^2 N_B)}$ , where  $N_B$  is the doping concentration on the more lightly doped side of an abrupt junction. The Debye length of the emitter-base junction in this device is  $4.1 \text{ nm}$  and  $13 \text{ nm}$  for the collector-base junction. The depletion width of a junction is given by [6]  $W = L_D \sqrt{2[q(V_{bi} - V_{apl}) / (k_B T) - 2]}$ , where  $V_{bi}$  is the built-in voltage and  $V_{apl}$  is the applied bias. The emitter-base junction has a depletion width of  $0.036 \mu\text{m}$ . The collector-base junction is  $0.10 \mu\text{m}$  when no bias is applied and  $0.22 \mu\text{m}$  when  $V_E = V_B = 0\text{V}$  and  $V_C = 3.0\text{V}$ .

The metallurgical junction width from the bottom of the emitter to the bottom of the base region is  $0.103 \mu\text{m}$ . The calculated electron depletion region (the base width plus the collector-base depletion, which is assumed to take place entirely in the collector) is  $0.208 \mu\text{m}$  for the zero bias case while it is  $0.327 \mu\text{m}$  for the biased case. Using a threshold of a factor of two less than the doped concentration as the edge of the depletion region, the results from the thermal equilibrium solution gave an electron depletion region of  $0.195 \mu\text{m}$  while the depletion calculation gave  $0.303 \mu\text{m}$ . These compare favorably to the analytically calculated results; however, agreement will not be exact due to three dimensional effects and the error in assuming all of the depletion occurs on the more lightly doped side of the junction.

The width of the undepleted base decreased from  $0.103 \mu\text{m}$  in the charge neutral case to  $0.072 \mu\text{m}$  at thermal equilibrium. When the final depletion correction including the bias was added, the base width was  $0.059 \mu\text{m}$ . These results are similar to experimental measurements [7].

The comparison of the charge-neutral approximation  $u_{cn}$  and the multi-dimensional depletion approximation  $u_{depl}$  demonstrates clearly the superiority of the computational depletion approximation. The strong rounding of the electron depletion region in our device with an exactly rectangular doping profile, demonstrates the need for a 3-D calculation. Table 1 reflects the linear computational complexity of the calculation.

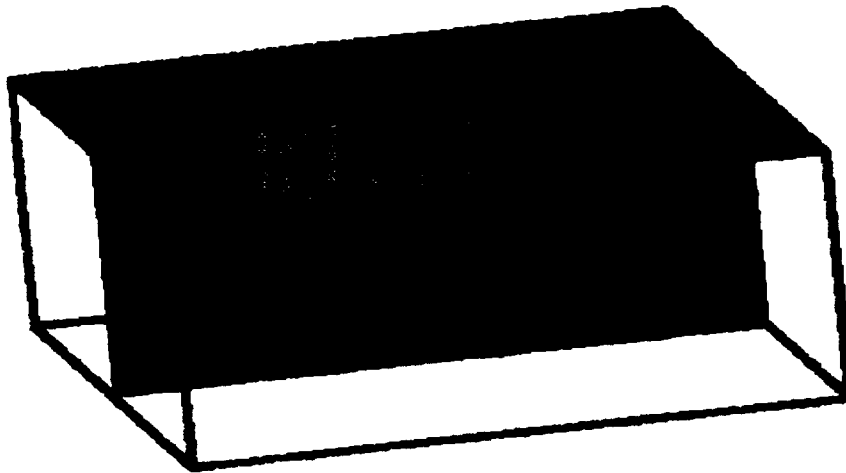


Figure 1: Charge neutral solution. The light area of both planes is the base region while the exterior dark region is the collector and the interior dark region is the emitter. This is the same orientation as the above figure: looking up from slightly below the device. The contacts are on the top plane.

## References

- [1] Michael Holst. *Multilevel Methods for the Poisson-Boltzmann Equation*. PhD thesis, Numerical Computing Group, Department of Computer Science, University of Illinois at Urbana-Champaign, 1993.
- [2] Michael Holst and Faisal Saied. Multigrid solution of the Poisson-Boltzmann equation. *Journal of Computational Chemistry*, 14(1):105–113, 1993.
- [3] Richard S. Muller and Theodore I. Kamins. *Device Electronics for Integrated Circuits*. John Wiley and Sons, New York, second edition, 1986.
- [4] S. M. Sze, editor. *High-speed Semiconductor Devices*. Wiley-Interscience, New York, 1990.
- [5] D. D. Tang and Paul M. Solomon. Bipolar Transistor Design for Optimized Power-Delay Logic Circuits. *IEEE Journal of Solid-State Circuits*, SC-14(4):679–684, Aug 1979.
- [6] S.M. Sze. *Physics of Semiconductor Devices*. Wiley-Interscience, New York, second edition, 1981.
- [7] Joachim N. Burghartz, Jack Yuan-Chen Sun, Carol L. Stanis, Siegfried R. Mader, and James D. Warnock. Identification of Perimeter Depletion and Emitter Plug Effects in Deep-Submicrometer, Shallow-Junction Polysilicon Emitter Bipolar Transistors. *IEEE Transactions on Electron Devices*, 39(6):1477–1489, Jun 1992.



Figure 2: Thermal equilibrium solution. The lighter area is the region of the base which is not depleted in the thermal equilibrium case. The device is  $1\ \mu m$  on a side.

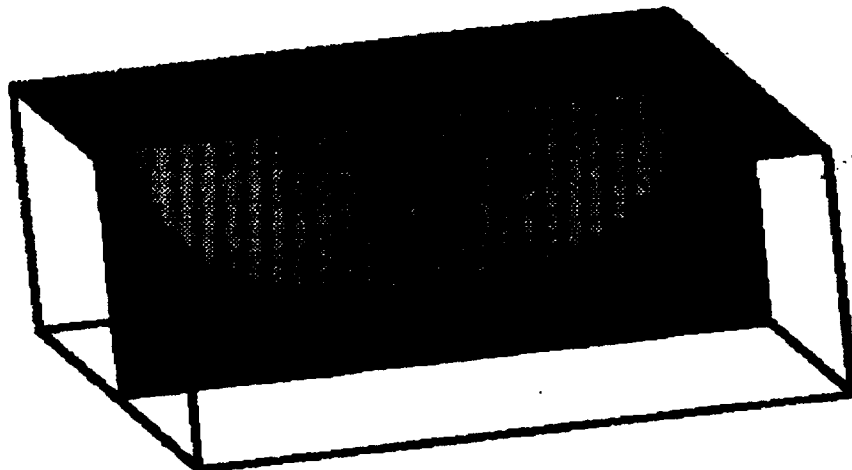


Figure 3: Depletion approximation solution. The small light area is the undepleted region of the base when the contact potential is applied.